INTERNATIONAL JOURNAL OF ENERGY STUDIES

e-ISSN: 2717-7513 (ONLINE); homepage: https://dergipark.org.tr/en/pub/ijes

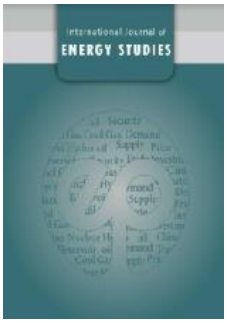

Research Article

Int J Energy Studies, 2021;6(2):95-125

Received: 22 Sep 2021
Revised: 26 Oct 2021
Accepted: 01 Nov 2021

Numerical modeling of momentum, heat transfer and combustion mechanisms of non-premixed swirling flame movement inside a cylindrical combustor

Fatih Eker[a], İlker Yılmaz[b,*]

[a] *Graduate School of Natural and Applied Sciences, Erciyes University, Kayseri, 38039, Turkey, ORCID Number: 0000-0001-9937-152X*

[b] *Department of Airframes and Powerplants, Faculty of Aeronautics and Astronautics, Erciyes University, Kayseri, 38039, Turkey, ORCID Number: 0000-0001-7956-7752*

*(*Corresponding Author: iyilmaz@erciyes.edu.tr)*

Highlights

- 3D RANS simulations of turbulent combustion in the Harwell furnace have been performed by being defined periodicity.
- Realizable k-epsilon and SST k-omega successfully predict temperature and velocity field.
- Standard k-epsilon has been more successful than other turbulence models in capturing temperature values in the centerline.
- In general, FR/EDM-4 step presents results in agreement with experimental data for temperature field.
- SDFM-GRI Mech 3 has failed to predict velocity field towards the exit of the furnace.

You can cite this article as: Eker, F., Yılmaz, İ. "Numerical modeling of momentum, heat transfer and combustion mechanisms of non-premixed swirling flame movement inside a cylindrical combustor", *International Journal of Energy Studies* 2021:6(2);95-125.

ABSTRACT

This study presents a numerical investigation of momentum, heat transfer, and combustion mechanisms of non-premixed swirling flame movement of a cylindrical combustion chamber. Fluent, a commercial CFD software, has been used in calculations. Combinations created with different turbulence models, combustion models and reaction mechanisms have been compared with experimental results. Realizable k-epsilon and FR/EDM-4 step combination have increased capacity to predict reacting flow, resulting in better accuracy. FR/EDM-4 step has provided much more reliable results than other scenarios, especially the Flamelet model used with a detailed chemical mechanism. In addition, the effect of radiation heat transfer on the temperature field has been investigated. Considering radiation heat transfer causes an increase in heat transfer from the combustion chamber, which provides desired agreement with experimental results. Finally, the effects of different Schmidt numbers on temperature and velocity fields have been investigated. Schmidt number has not caused significant changes in the velocity field. Also, as the Schmidt number increases, it has been observed that the flame temperatures decrease to a certain extent in the combustion chamber.

Keywords: *Combustion modeling, Turbulence modeling, Turbulent non-premixed flames, Combustion engineering, Radiation heat transfer*

1. INTRODUCTION

Combustion problems encompass many phenomena such as turbulence, fluid mechanics, multiphase flow, heat transfer, radiation, pollution and chemical reactions.

Almost all flows we encounter in daily life and engineering applications are turbulent. Therefore, CFD has focused on these flows, where turbulence is dominant. Although the physics of turbulence is not fully understood, turbulence can be modeled with satisfactory accuracy through numerical simulations. Due to affordable computation requirements in turbulence modeling, the Reynolds-averaged Navier-Stokes (RANS) approach has been the backbone of industrial computational fluid dynamics applications for the past few decades. In addition RANS approach is constantly employed in steady-state flows where detailed instantaneous flow does not need to be modeled. Although large eddies are modeled in the RANS approach, the Large Eddy Simulation (LES) approach directly captures fluid packages containing large eddies in detail. Although the RANS approach leads to a marked reduction in computation time, the LES approach gives more accurate results [20]. However, the LES approach is too costly to be a conventional method for the industry due to the computing power it demands [4].

Combustion models and reaction mechanisms, the most critical phenomena in reacting flows, directly affect the temperature field. Hence, selecting suitable combustion models and reaction mechanisms for simulations of combustion systems plays a vital role in precisely estimating velocity field in addition to high-temperature regions. This situation is the main focus of the study.

Thermal radiation in gaseous media is indispensable in high-temperature chambers, such as industrial furnaces and aero-engine combustion chambers, even under non-soot conditions. Increasing attention to high-temperature processes has laid the groundwork for evaluating the effect of radiation heat transfer [5].

Many researchers and combustion engineers have conducted scientific scrutinies to numerically model momentum, heat transfer and combustion mechanisms in reacting flows.

Silva et al. [1] studied the effects of radiation heat transfer from natural gas combustion in a cylindrical combustion chamber. They used the weighted-sum-of-gray-gases model to account for gas absorption coefficients. When radiation heat transfer was included, it was stated to increase heat transfer from hot gases to combustor outside. In addition, they indicated that radiation heat transfer was more critical than convection heat transfer in most combustion chamber areas. Jiang et al. [2] investigated the effect of turbulent Prandtl/Schmidt numbers ranging from 0.25 to 0.85 on temperature and velocity fields by modeling a propane flame in a combustion chamber. When they compared numerical results obtained with experimental results, they found that the Schmidt number had an insignificant effect on the velocity field and substantially affected the temperature field and temperature profile on combustion chamber walls. Yang et al. [3] and Solmaz et al. [4] made use of realizable k-epsilon and finite rate/eddy dissipation, respectively, as the turbulence and combustion model in turbulent combustion simulations they conducted. Keremida et al. [5] numerically modeled a turbulent natural gas flame in a cylindrical combustion chamber. They compared experimental data to two different radiation models - the discrete transfer and the six flux. They argued that six flux was more feasible in industrial combustion chambers. In addition, considering radiation heat transfer, they emphasized that it was crucial in coherence with experimental data. Yılmaz [6] found that different swirl numbers in a combustion chamber seriously affected recirculation zones, velocity distributions and flame temperatures. The author employed a combination of standard k-epsilon, eddy dissipation and P1 as the turbulent, combustion and radiation model in this work, respectively. Bahramian et al. [7] modeled methane-air flame in a gas turbine combustion chamber. They used re-normalization group k-epsilon as the turbulence model. They argued that eddy dissipation concept predicted more accurately temperature field than finite rate/eddy dissipation as the combustion model. Hosseini et al. [8] investigated the effects of different swirl numbers on methane-air diffusion flame. They found that as the swirl number increased, high-temperature regions disappeared, and a uniform distribution in heat transfer flux along the combustor axis arose. Silva et al. [9] used different combustion models and reaction mechanisms to model turbulent non-premixed natural gas combustion in a cylindrical combustion chamber. They used the discrete transfer radiation method to model radiation heat transfer and the weighted-sum-of-gray-gases model to consider gas absorption coefficients. They used standard k-epsilon as the turbulence model.

With the 2-step Westbrook Dryer global reaction mechanism and GRI-Mech 3.0 chemical mechanism, they employed three different combustion models - eddy break-up (EBU)/arrhenius, steady laminar diffusion flamelet (SLDF) and eddy break-up. They found that EBU/arrhenius was better at predicting flame temperatures than sophisticated SLDF. Saygin et al. [10] conducted a numerical study by employing a combination of realizable k-epsilon, discrete ordinates and hybrid eddy break-up in order to model reacting flow in a gas turbine combustion chamber. They investigated the effects of radiation heat transfer and different Schmidt numbers on temperature area and liner of the combustion chamber. They suggested that estimates obtained by considering radiation heat transfer presented more accurately liner temperatures. Finally, they said that as the Schmidt number decreased, liner temperatures raised in the primary region and declined in the secondary region. Benim et al. [11] investigated isothermal swirling flow in a model combustion chamber experimentally and numerically. They observed that results obtained from the Unsteady Reynolds-averaged Navier-Stokes approach were not as good as results obtained from the Large Eddy Simulation (LES) approach in general. However, they discovered that the reynolds stress model (RSM) gave better results in some parts of the combustion chamber where the LES approach was insufficient. In addition, they emphasized that RSM was more compatible with experimental results than the shear stress transport model. Yang et al. [12] and İlbaş et al. [13] examined reacting flow inside a non-premixed cylindrical combustion chamber with ANSYS Fluent software. They claimed that the probability density function/mixture fraction combustion model presented much more reliable results in predicting flame temperatures, especially compared to the eddy dissipation model. While Yang et al. employed modified standard k-epsilon as the turbulence model, others chose realizable k-epsilon. Benim et al. [14] conducted a numerical study of turbulent swirling flame in a gas turbine combustion chamber employing Large Eddy Simulation (LES) and Unsteady Reynolds-averaged Navier-Stokes (URANS) approaches. They processed the Schmidt number as 0.7 in this study. LES-laminar flamelet method (LFM), LES-eddy dissipation concept (EDC), URANS-laminar flamelet method (LFM) were combinations created within the scope of the investigation. They observed that combinations employed with LES produced better accuracy than those employed with URANS. However, they discovered that the URANS approach was more useful in computing time. For LES, they stated that EDC presented similar overall accuracy compared to LFM, even slightly better.

In addition, it has been observed that LFM requires a shorter computation time than EDC, which makes LFM more alluring than EDC for combustion chambers that demand high element numbers or sophisticated reaction mechanisms. Yılmaz et al. [15] evaluated the effects of different turbulence and radiation models on temperature-velocity profiles and species concentration profiles to numerically model propane-hydrogen diffusion flames in various blends and compared results obtained with experimental data. They applied re-normalization group (RNG) k-epsilon and reynolds stress model as turbulence model and P1 and discrete transfer model as radiation model. As a result, they preferred RNG k-epsilon and P1 to carry out the fuel blending study because of the desired compatibility with experiment results. Garcia et al. [16] utilized different reaction mechanisms such as UC-San Diego, GRI 3.0 and DRM19 with the eddy dissipation concept and the steady diffusion flamelet combustion models to analyze turbulent combustion in a combustion chamber. They discussed outcomes by comparing temperature profiles obtained from numerical analysis with experimental data. İlbaş et al. [17] conducted a numerical study on hydrogen combustion with low-calorific value syngases. They employed a combination of the standard k-epsilon turbulence model, probability density function/mixture fraction combustion model and P1 radiation model to model turbulent combustion in the combustor they designed. Tyliszczak et al. [18] validated consequences obtained from numerical analysis with experimental data employing k-epsilon/Smooke mechanism, Large Eddy Simulation (LES)/GRI-2.11 and k-epsilon/GRI-2.11 combinations. They found that chemical kinetics had a more substantial effect on conclusions than the turbulence model. Yılmaz et al. [19] numerically investigated the effects of different turbulence models on combustion and emission characteristics in a micro-cylindrical combustion chamber. They discovered that the re-normalization group k-epsilon turbulence model produced even harmonious outcomes with experimental data. In addition, they stated that the reynolds stress turbulence model is inadequate to predict centerline temperatures.

Based on the above studies, the choice of turbulence model, combustion model and reaction mechanism plays a critical role when modeling a combustion chamber. 3D simulations of the Harwell combustion chamber have been conducted in this study, unlike studies in the literature. Flow volume has periodically been resolved. Flow volume corresponding to 360/6° slice of the combustion chamber has been created through SpaceClaim. The effects of various turbulence models on temperature and velocity fields have been investigated.

The suitability of shear stress transport k-omega and standard k-omega for the combustion chamber has been examined. The combination that increases the capacity to predict flame temperatures using different combustion models and different reaction mechanisms has been scrutinized. GRI Mech 3.0, a detailed reaction mechanism, has been applied with the steady diffusion flamelet model. 4-step and 3-step reaction mechanisms have been employed with the finite rate/eddy dissipation model. The purpose of these combinations is to determine the scenario that best predicts the temperature and velocity field for the industrial combustion chamber. In addition to these studies, the effects of scenarios consisting of different turbulent Schmidt numbers on temperature and velocity fields have been studied. Finally, the effect of radiation heat transfer on the temperature field has been investigated using the discrete ordinates (DO) model. Temperature-velocity contours and profiles have been created systematically for all studies and then the outcomes have been interpreted by comparing with experimental data [6].

2. GEOMETRY DEFINITION

Harwell furnace, the cylindrical combustion chamber with a diameter of 0.3 m and a length of 0.9 m, is shown in Figure 1. Air is supplied from an annular jet on the outside, and also a swirling diffusion flame is produced by two separate jets having the same axis to make happen combustion [5].

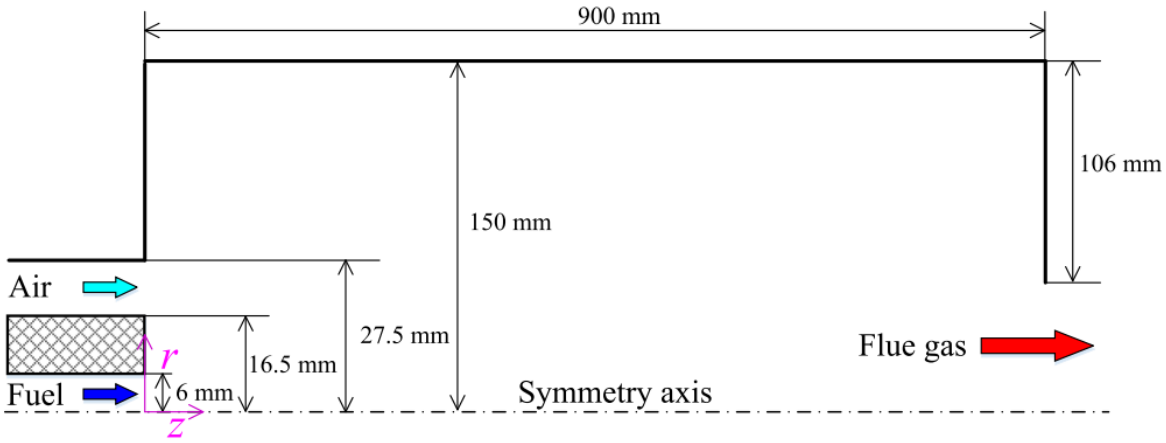

Figure 1. Combustion chamber geometry [12].

3. MESH DETAILS

Solution mesh presented in Figure 2 has been produced with the help of polyhedral cells by using Ansys Meshing software. Mesh structure consisting of polyhedral cells contains approximately 4-5 times fewer elements than mesh structure consisting of tetrahedral cells. Polyhedral cells also increase mesh quality and offer ease of convergence. In addition to polyhedral cells in the combustion chamber, thin-layered cells called boundary layer mesh have been produced to examine the boundary layer in detail. Smaller cells have been preferred at the inlet of the combustion chamber to enhance flow and mix better air and fuel. Three different computational meshes -coarse, medium and fine- have been created to achieve grid independence.

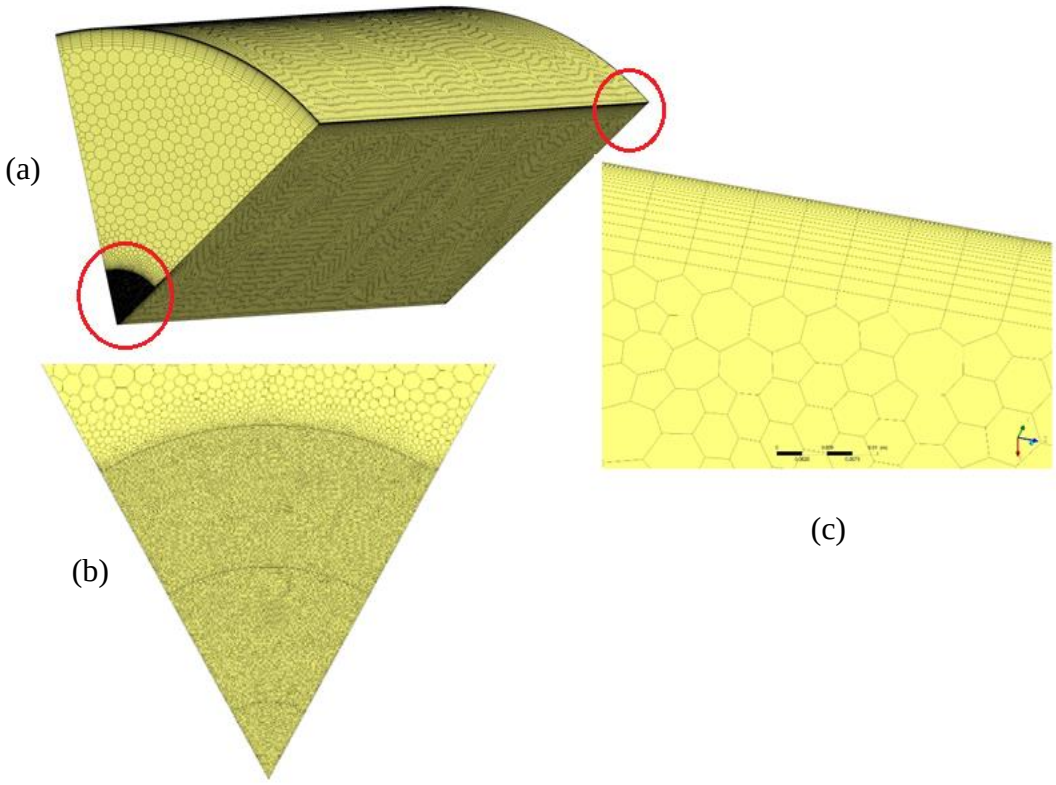

Figure 2. For medium-mesh ; (a) general view of the combustion chamber, (b) polyhedral cells in the fuel-air inlet and (c) boundary layer composed of thin-layered cells.

Cell numbers are 24722, 268288 and 597029, respectively. The average y+ values on the walls of these computational meshes are 6.08, 1.48, 1.25, respectively. Salim et al. [21] have kept the y+ value smaller than 5 for detailed resolution of the viscous sub-layer. Accordingly, the y+ value has been kept less than 5 in medium-mesh and fine-mesh in the study.

4. BOUNDARY CONDITIONS AND SOLVER SETTINGS

Wall temperatures have been processed as 400 K, given that combustion chamber walls are completely water-cooled. In addition, a value of 0.8 has been processed for the emissivity ratio on walls, which is an essential parameter in modeling the radiation heat transfer. Finally, absorption and scattering coefficients have been employed as 0.5 m^{-1} and 0.01 m^{-1}, respectively [3]. Table 1 shows boundary conditions for the combustion chamber.

Table 1. Inlet conditions and fluid properties for fuel-air [6].

Boundary conditions	Fuel	Air
Axial velocity (m/s)	15	12.8
Radial velocity (m/s)	0	0
Turbulent kinetic energy (m^2/s^2)	2.26	1.63
Dissipation rate of turbulence (m^2/s^3)	1131.8	692
Temperature (K)	295	295
Swirl number	0	0.4

Utilizing the cell-centered finite volume method to discretize continuity, momentum, energy and species transport equations in numerical studies, Ansys Fluent has been employed. Detailed information about governing equations can be found in Ref. [26]. The following can be stated about the combustion models used in the paper. For Figure 4, while eddy dissipation ignores chemical kinetics and employs only mixing rate parameters in the reactions dialog box, values for rate exponent and arrhenius rate parameters are involved in the database, when finite rate/eddy dissipation model is employed. To use the steady diffusion flamelet model, chemical kinetic mechanism and thermodynamic data in CHEMKIN format must be defined, and a flamelet file must be generated [29]. It can be said that the discrete ordinates model employed in radiation modeling is the most computationally expensive and comprehensive and accurate. Although P1, frequently used in modeling radiation heat transfer, offers reasonable accuracy for moderate cost, it is only used when the optical thickness is greater than 1 [27]. The following equation can give optical thickness.

$$\text{Optical Thickness} = (a + \sigma_s)\, L$$

a, σ_s and L expressions signify absorption coefficient, scattering coefficient, and a typical distance between 2 opposing walls [27]. More detailed information on this can be found in Ref. [27]. In addition, turbulence, combustion and radiation model equations used to model reacting flow within the scope of the paper can be attained in Ref. [25].

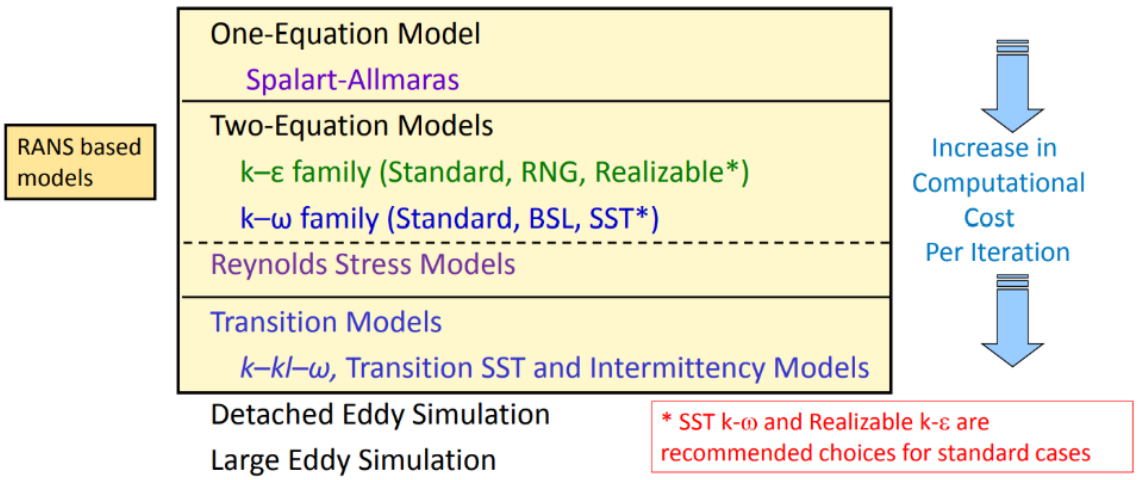

Figure 3. Turbulence models available in Fluent [28].

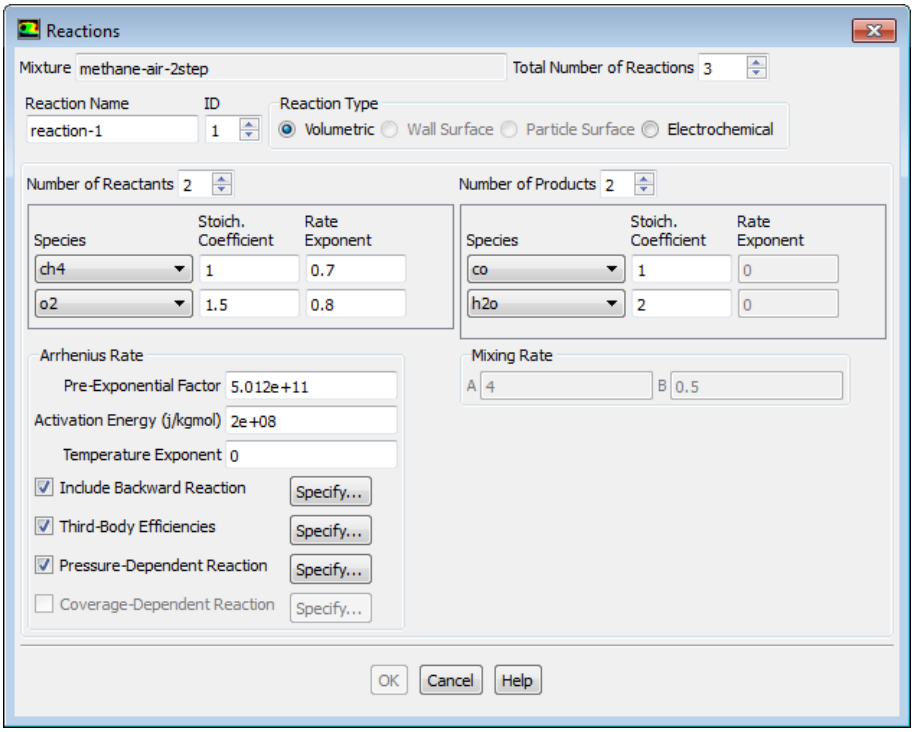

Figure 4. The reactions dialog box [29].

CFD calculations have been run by using 4 CPU cores. Solver settings used for both mesh independence study and further studies are presented in Table 2. Detailed information about chemical reactions is shown in Table 3, Table 4 and Table 5. A, b and E_a expressions in Table 3 and Table 4 signify pre-exponential factor, temperature coefficient and activation energy.

For pressure-velocity coupling in numerical calculations of the combustor, while the SIMPLE algorithm was applied in Ref. [6], [8] and [12], the Coupled algorithm was used in the current study.

Table 2. Detailed solver settings.

Models	Descriptions
Solver type	Pressure-based
Time	Steady
Gravity	On
Solution methods	Coupled scheme for pressure-velocity coupling; Second upwind scheme for pressure equation; Second order upwind scheme for other equations
Pseudo transient	On
Turbulence model	Realizable k-epsilon
Near-wall treatment	Enhanced wall treatment
Combustion model	Finite rate/eddy dissipation
Reaction mechanism	4-step reaction mechanism shown in Table 4
Radiation model	Discrete ordinates with 2 x 1 angular discretization; 1 energy iteration per radiation iteration
Turbulent Schmidt number	0.7
Mesh interfaces	360/6°
Converge criterion	10^{-3} for continuity equation, and 10^{-6} for all other equations

Table 3. Parameters processed to generate combustion chemistry using a 3-step reaction mechanism [22].

No.	Reaction	A	b	E_a [cal/mol]	Reaction orders
1	$CH_4 + 1.5O_2 \rightarrow CO + 2H_2O$	2e+15	0	35000	$[CH_4]^{0.9}\,[O_2]^{1.1}$
2	$CO + 0.5O_2 \rightarrow CO_2$	2e+09	0	12000	$[CO]\,[O_2]^{0.5}$
3	$CO_2 \rightarrow CO + 0.5O_2$	8.1104e+10	0	77194	$[CO_2]$

Table 4. Parameters processed to generate combustion chemistry using a 4-step reaction mechanism [23].

No.	Reaction	A	b	E_a [kj/mol]	Reaction orders
1	$CH_4 + 0.5O_2 \rightarrow CO + 2H_2$	7.82e+13	0	30.0e+03	$[CH_4]^{0.5}\,[O_2]^{1.25}$
2	$CH_4 + H_2O \rightarrow CO + 3H_2$	0.30e+12	0	30.0e+03	$[CH_4]\,[H_2O]$
3	$H_2 + 0.5O_2 \rightarrow H_2O$	1.21e+18	-1	40.0e+03	$[H_2]^{0.25}\,[O_2]^{1.5}$
4	$CO + H_2O \rightarrow CO_2 + H_2$	2.75e+12	0	20.0e+03	$[CO]\,[H_2O]$

Table 5. Mass fraction of species at fuel and air inlet boundary condition.

	Fuel					Air	
	CH_4	CO_2	C_3H_8	N_2	C_2H_6	O_2	N_2
EDM-1 step	1	-	-	-	-	0.2315	-
FR/EDM-3 step	0.997	0.003	-	-	-	0.2315	-
FR/EDM-4 step	1	-	-	-	-	0.2315	-
SDFM-GRI Mech 3	0.966	0.003	0.001	0.013	0.017	0.2315	0.7685

5. RESULTS AND DISCUSSION

5.1. Grid independence

To discuss the effects of solution mesh on results, temperature and velocity profiles have been examined through observation lines formed as four vertical (Line 2, Line 3, Line 4, Line 5) and one horizontal (Line 1) taken from the midplane of the combustion chamber.

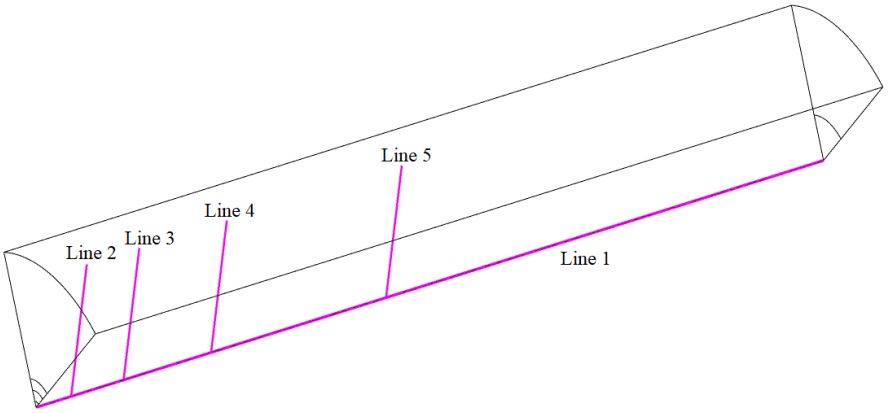

Figure 5. Horizontal and vertical lines taken from the central section of the combustor.

In addition to velocity and temperature profiles, local contour representations of temperature and velocity fields have also been made through a plane taken from the central section of the combustion chamber. When temperature and velocity profiles in Figure 7 are examined, it is seen that all of the computational meshes follow a similar trend. Still, it is observed that medium-mesh and fine-mesh are more compatible with each other in oscillation zones. For temperature contours in Figure 6, it is seen that coarse-mesh has formed a thicker flame structure in the radial direction and has presented a relatively different temperature distribution in small recirculation zone compared to medium-mesh and fine-mesh.

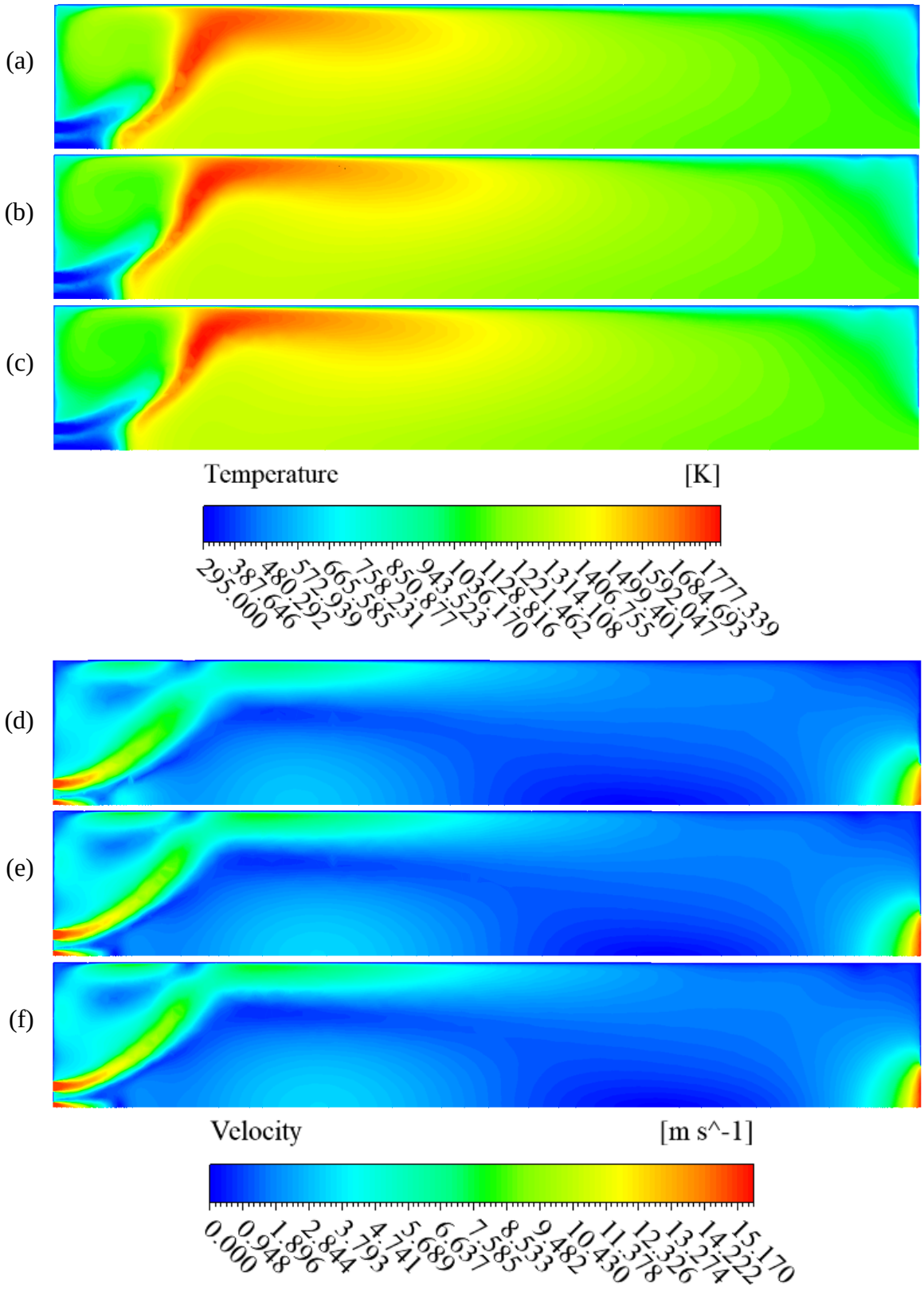

Figure 6. Contours showing temperature fields for (a) coarse, (b) medium, (c) fine mesh and velocity fields for (d) coarse, (e) medium, (f) fine mesh.

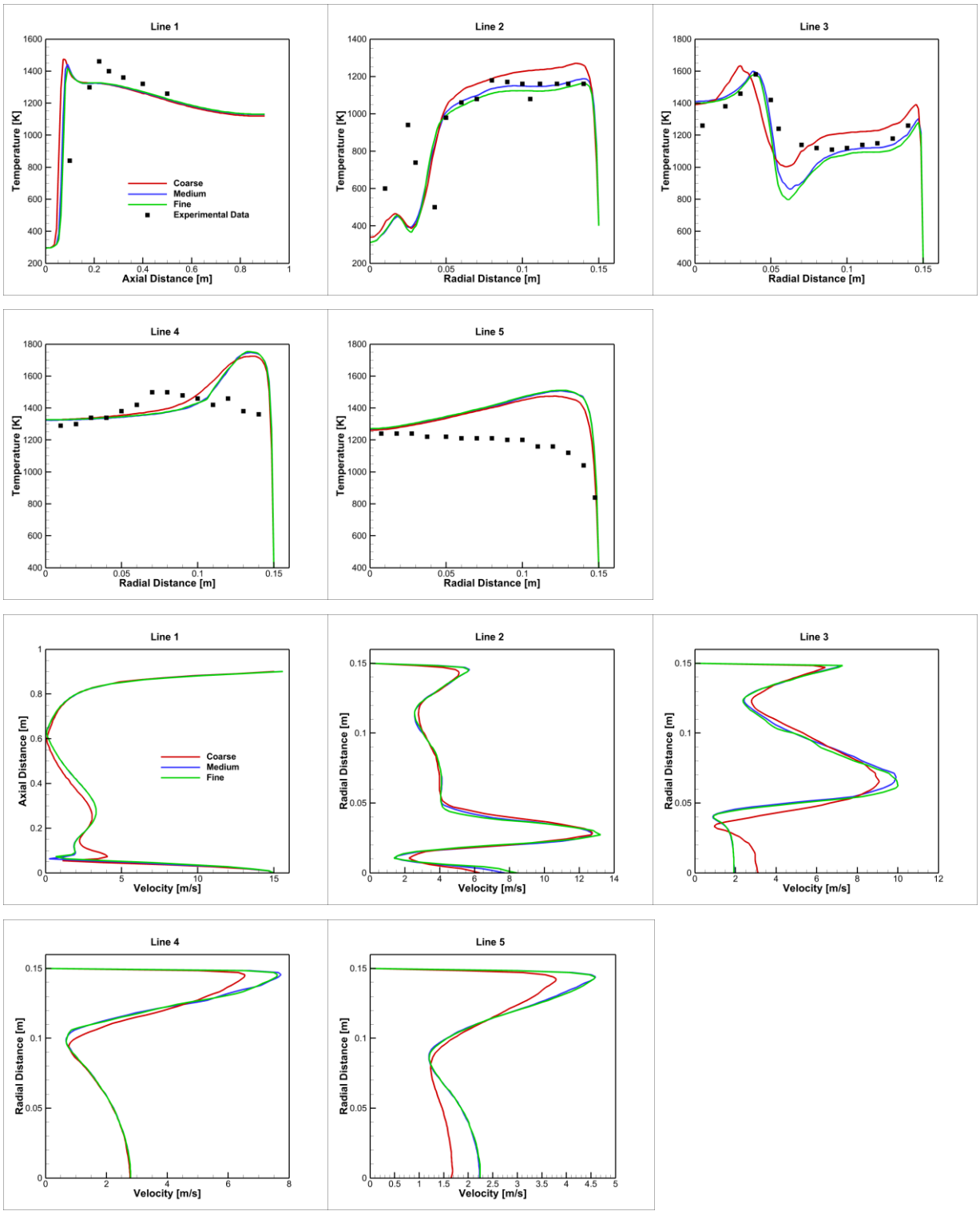

Figure 7. Temperature and velocity profiles on horizontal and vertical lines created for independence study from computational mesh.

For velocity contours in Figure 6, it is observed that coarse-mesh offers by differing slightly recirculation zones and flow separations in addition to velocity distributions towards the outlet of the combustion chamber, especially.

Considering that medium-mesh and fine-mesh give results much closer to each other in temperature and velocity fields on contours, just like temperature and velocity profiles, it is concluded that medium-mesh is independent of solution mesh. In addition, when considering simulation times and computer resources, it has been decided that it is more appropriate to use medium-mesh in the future.

5.2. Turbulence modeling study

In the turbulence modeling study, five different models have been studied: standard k-epsilon, re-normalization Group (RNG) k-epsilon, realizable k-epsilon, shear stress transport (SST) k-omega, and standard k-omega model. Temperature-velocity profiles on horizontal and vertical lines and temperature-velocity contours on midplane have been presented to research the effects of different turbulence models on the flow field. The finite rate/eddy dissipation model (FR/EDM) and the 4-step reaction mechanism have been used, respectively, as the combustion model and reaction mechanism. Discrete ordinates (DO) has been used as the radiation model.

When looking at temperature profiles in Figure 8, it is observed that realizable k-epsilon, SST k-omega, and standard k-epsilon are much more compatible with each other. In the Line 1 graph, standard k-epsilon is closer to the experimental results than other turbulence models. It is seen that standard k-omega is generally insufficient to solve turbulence. RNG k-epsilon has given better results than standard k-omega. Realizable k-epsilon has created temperature distributions that provide the best approximation with experimental results, especially in Line 2 and Line 3 graphs.

For velocity profiles in Figure 8, it is observed that realizable k-epsilon and SST k-omega are more compatible with each other and exhibit more regular velocity distributions. RNG k-epsilon and standard k-omega are more oscillatory and irregular.

For temperature contours in Figure 9, standard k-epsilon has the broadest flame structure in the radial direction. It is observed that standard k-omega overestimates the flame region and reveals a structure with lower temperature values in small recirculation zone compared to results obtained from other turbulence models.

RNG k-epsilon is insufficient in predicting the flame region. Turbulence models that accurately solve the flame region are realizable k-epsilon and SST k-omega. For velocity contours in Figure 9, it appears that standard k-epsilon, RNG k-epsilon and standard k-omega cannot accurately predict recirculation zones and flow separations. Realizable k-epsilon and SST k-omega are highly compatible with each other.

Realizable k-epsilon is promising in terms of compatibility with experimental results, accuracy in predicting temperature-velocity fields and ease of convergence compared to SST k-omega. Because of these reasons and when considering recommendations in the literature well, it has been decided to be used realizable k-epsilon in subsequent analysis.

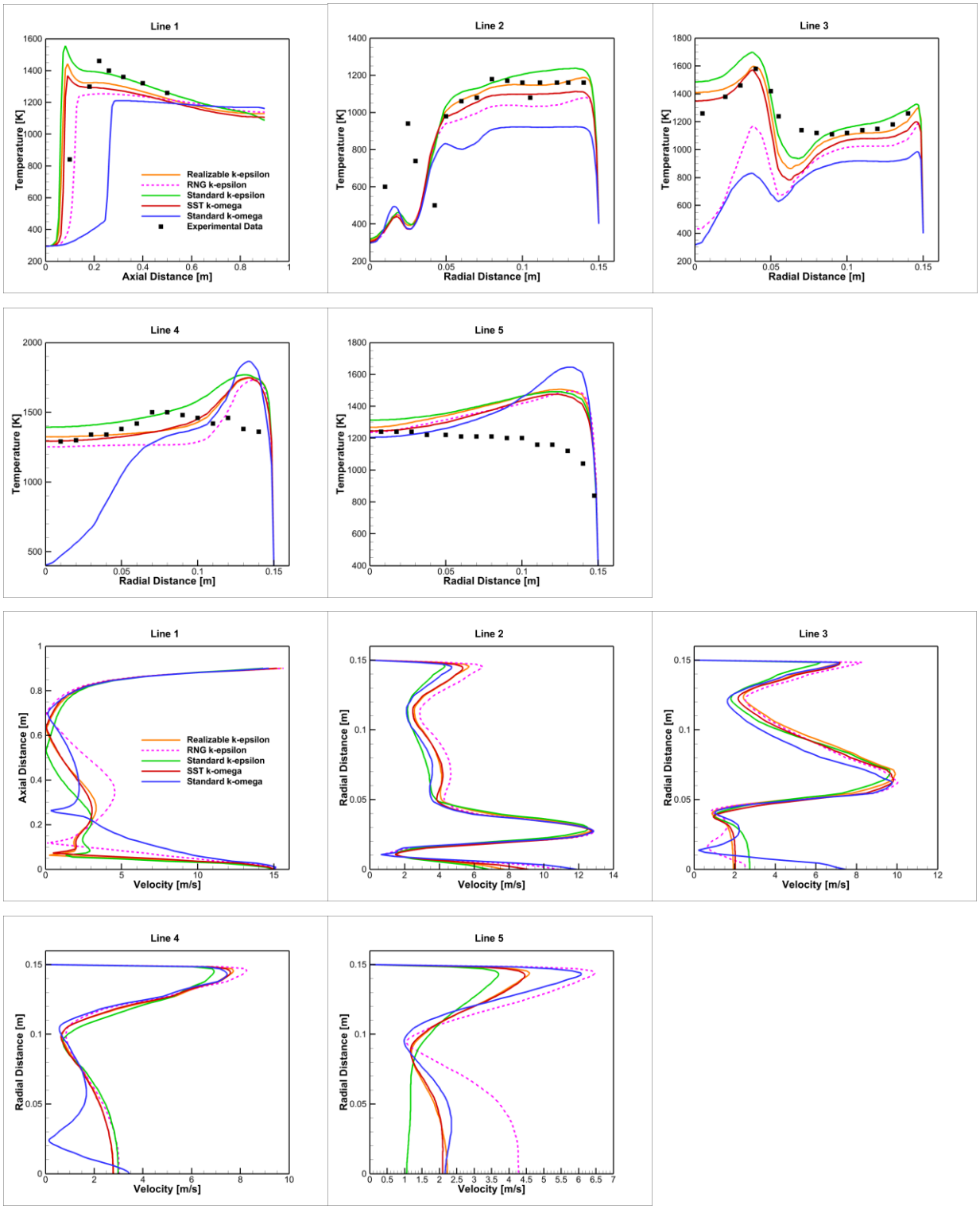

Figure 8. Temperature and velocity profiles on horizontal and vertical lines created for turbulence modeling study.

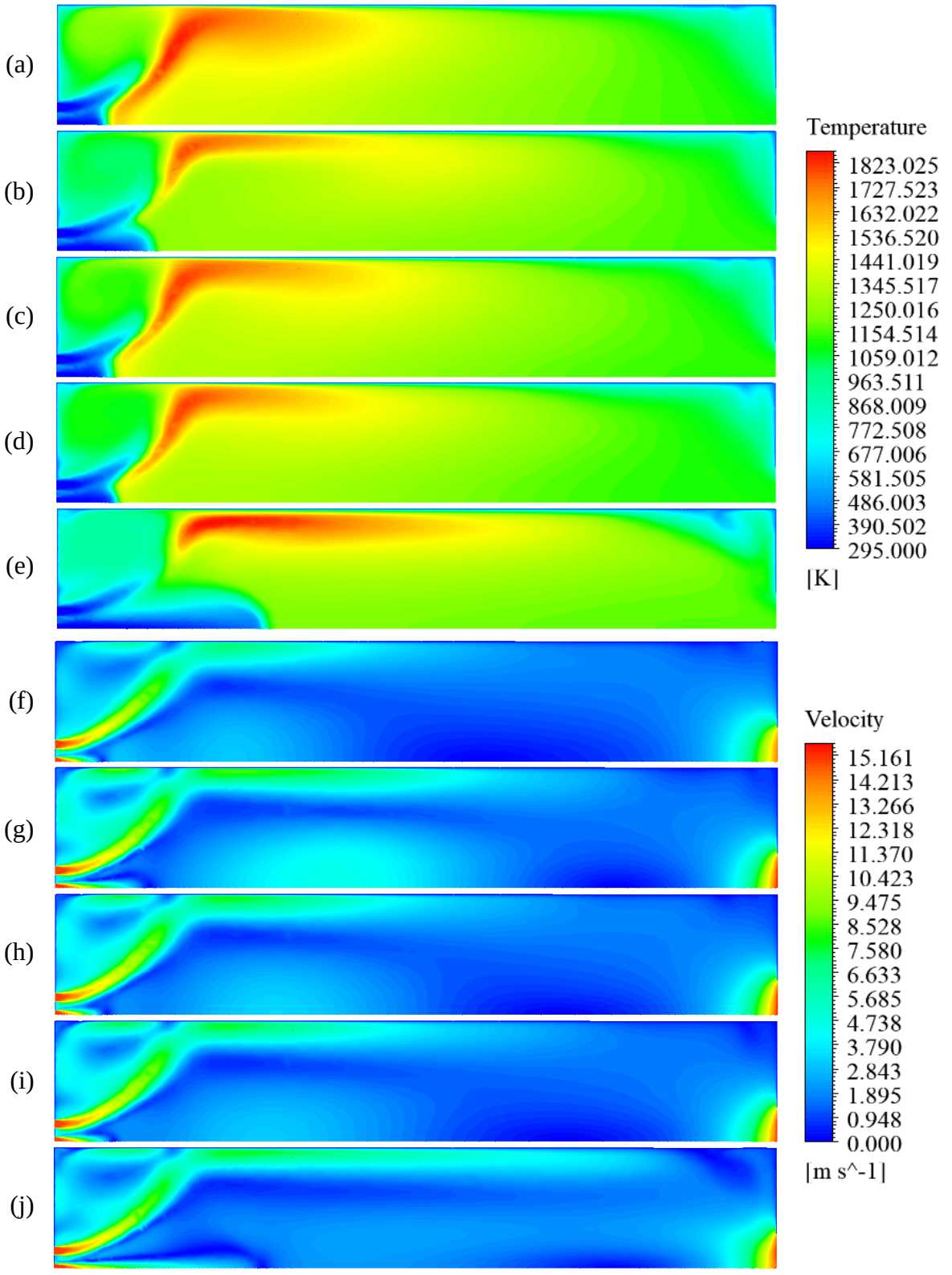

Figure 9. Contours showing temperature fields for (a) standard k-epsilon, (b) RNG k-epsilon, (c) realizable k-epsilon, (d) SST k-omega, (e) standard k-omega models and velocity fields for (f) standard k-epsilon, (g) RNG k-epsilon, (h) realizable k-epsilon, (i) SST k-omega, (j) standard k-omega models.

5.3. Combustion modeling study

For the combustion modeling study, four different combinations were created using different combustion models with different reaction mechanisms. In this section, temperature-velocity profiles and contours are examined as being in the turbulence modeling study.

Eddy dissipation (ED) was used with the 1-step reaction mechanism [25] included in Fluent by default. Finite rate/eddy dissipation (FR/ED) was used with the 3-step chemical mechanism proposed by Bibrzycki and Poinsot and the 4-step chemical mechanism proposed by Jones Lindstedt. Finally, steady diffusion flamelet (SDF) was used with a detailed chemical mechanism called GRI Mech 3.0 [24], which consisted of 53 species and 325 reaction mechanisms derived by Berkeley University. These combinations were briefly called EDM-1 step, FR/EDM-3 step, FR/EDM-4 step and SDFM-GRI Mech 3. Discrete ordinates (DO) was used as the radiation model. To examine the effects of different combinations on the flow field, temperature-velocity profiles on horizontal and vertical lines and temperature-velocity contours on midplane are presented.

When looking at temperature profiles in Figure 11, it stands out that FR/EDM-4 step is the most compatible with experimental results. For the Line 1 graph, EDM-1 step has offered a relatively more accurate temperature distribution than FR/EDM-4 step. However, EDM-1 step is insufficient in estimating temperature distributions in Line 2 and Line 3 graphs. Especially FR/EDM-4 step in Line 2 and Line 3 graphs is promising in terms of its closeness to experimental results. When focusing on the line 5 graph, temperature distributions constituted by FR/EDM-3 step are closer to experimental results compared to temperature distributions constituted by other combinations. However, when looking at graphs created with other observation lines, it is seen that this combination is insufficient to solve reacting flow. For the Line 1 graph, SDFM-GRI Mech 3 has highly low-temperature distributions. SDFM-GRI Mech 3 has created similar temperature distributions with EDM-1 step and FR/EDM-3 in other observation lines. Although a detailed chemical mechanism is used in the flamelet model, harmony desired with experimental results could not be achieved.

Velocity profiles in Figure 11 generally show the same trend in four different combinations. However, FR/EDM-4 step has presented a relatively different distribution in some parts of the combustion chamber compared to results obtained from other combinations for Line 1, Line 2 and Line 3 graphs.

When temperature contours in Figure 10 are examined, it is seen that EDM-1 step and FR/EDM-4 step present relatively similar high-temperature zones. FR/EDM-3 step has a quite different flame structure than other combinations and has created more limited high-temperature zones compared to results obtained from other combinations. Although the flame structure presented by the Flamelet model employed with a detailed chemical mechanism is similar to EDM-1 step and FR/EDM-4 step, this combustion model has created a flame zone where lower temperature distributions take place. EDM-1 step, FR/EDM 3 step and SDFM-GRI Mech 3 have created similar temperature distributions in small recirculation zone (Central Recirculation Zone, CRZ). Temperatures offered by the Flamelet model towards the combustion chamber exit are considerably lower than temperatures offered by other combinations.

Velocity contours in Figure 10 have formed similar structures as in velocity profiles in Figure 11; however, at the exit of the combustion chamber, FR/EDM-3 step and SDFM-GRI Mech 3 have created a more uniform velocity distribution. SDFM-GRI Mech 3 has differently predicted velocity distributions, especially large recirculation zone (Internal Recirculation Zone, IRZ) and flow separations, which causes a different pattern towards the exit of the combustion chamber compared to velocity distributions generated by other combinations to occur.

When modeling combustion in reacting flows, accurate estimation of high-temperature regions is crucial. Because it presents more reliable results besides its closeness to experimental results, the combustion model and reaction mechanism preferred in the paper is the combination created as FR/EDM-4 step. The richness of reaction number, long simulation time and incorrect estimation of velocity distributions towards the exit of the combustion chamber make SDFM-GRI Mech 3 disadvantageous for the combustion chamber. Particularly when considering the Line 1 graph, SDFM-GRI Mech 3 and FR/EDM-3 step have reduced capacity to predict temperature field.

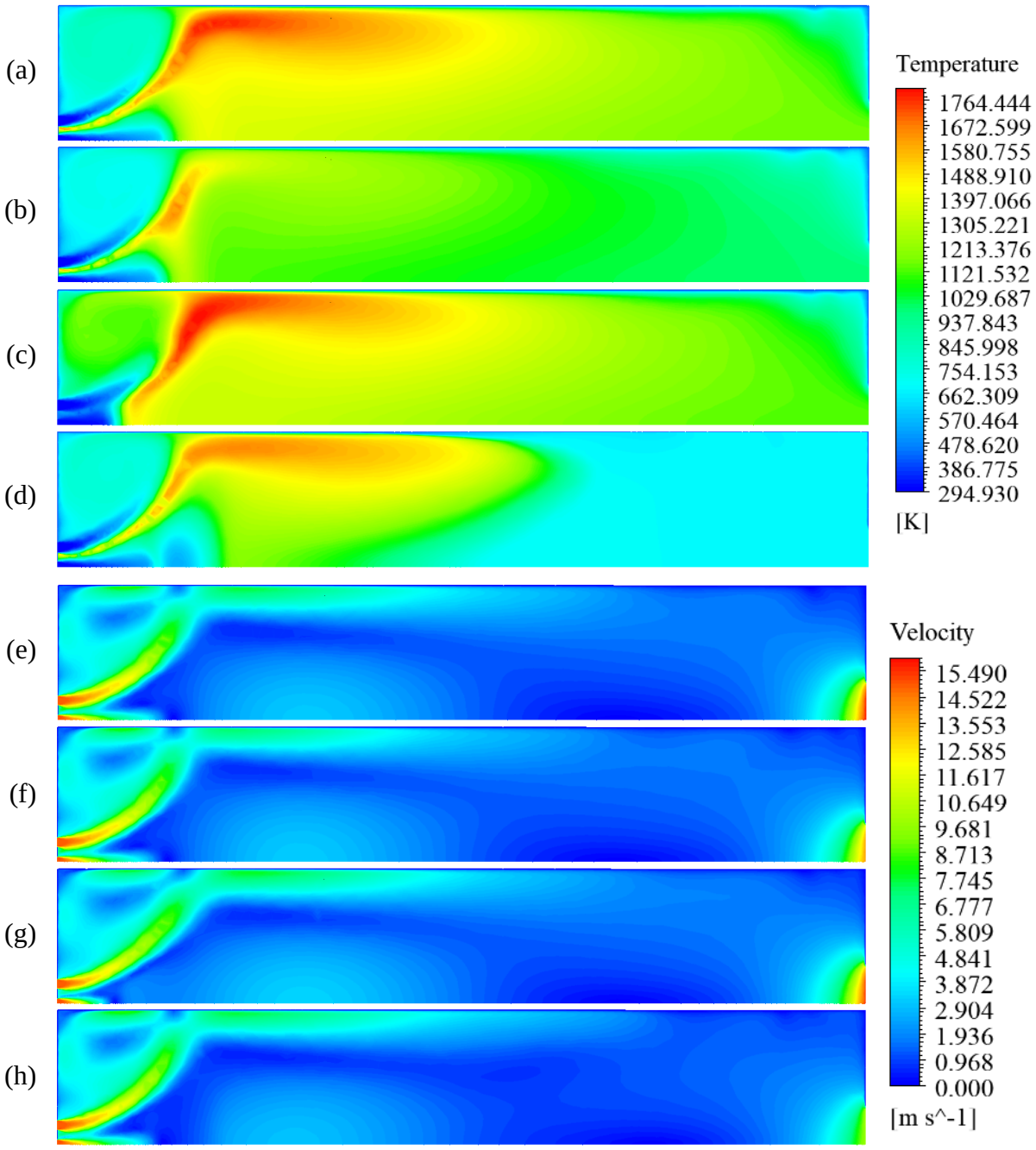

Figure 10. Contours showing temperature fields for (a) EDM-1 step, (b) FR/EDM-3 step, (c) FR/EDM-4 step, (d) SDFM-GRI Mech 3 and velocity fields for (e) EDM-1 step, (f) FR/EDM-3 step, (g) FR/EDM-4 step, (h) SDFM-GRI Mech 3.

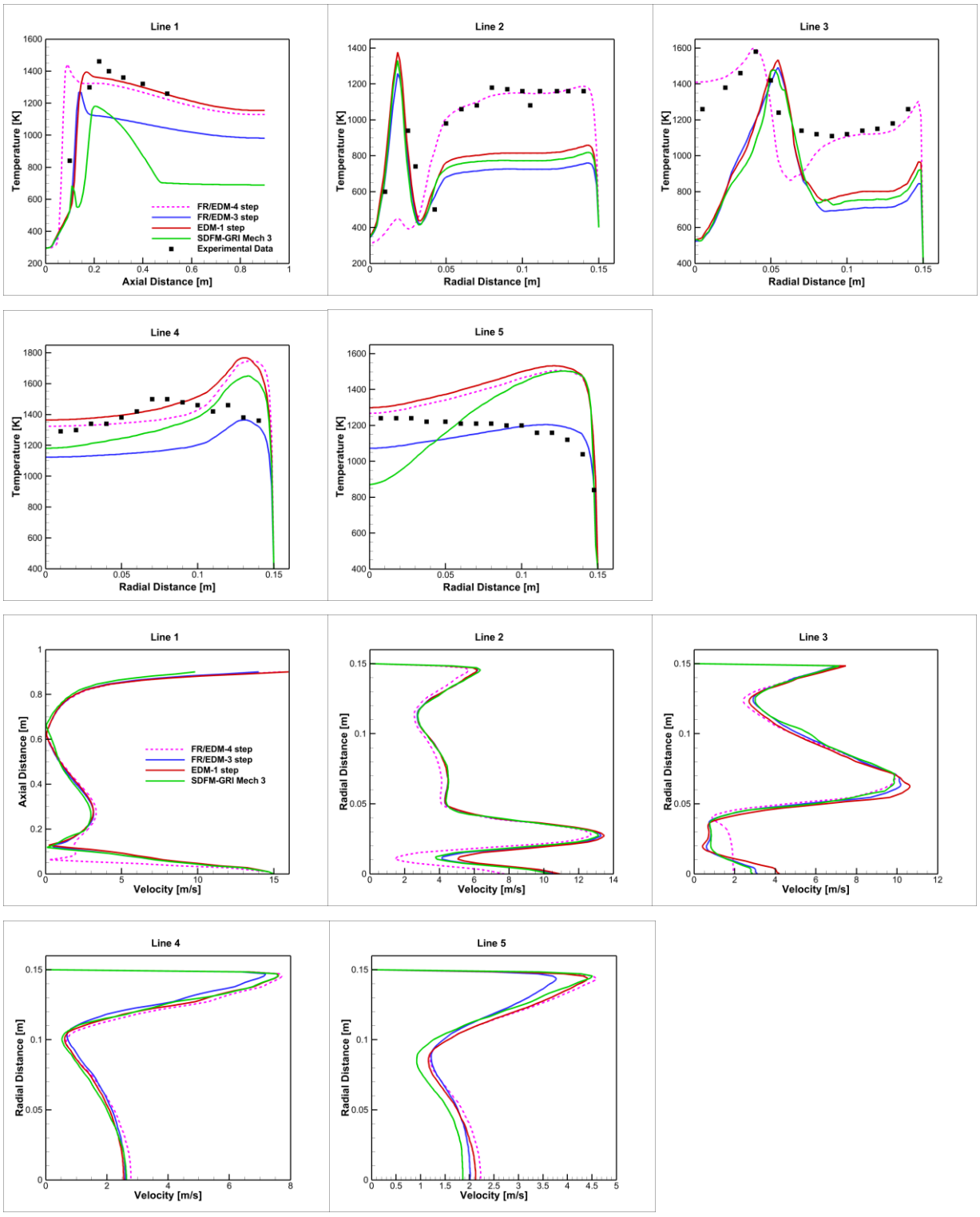

Figure 11. Temperature and velocity profiles on horizontal and vertical lines created for combustion modeling study.

5.4. Effect of Schmidt number

In Reynolds-averaged Navier-Stokes (RANS) simulations, turbulent Schmidt and Prandtl numbers play an essential role in determining mixing fraction, species and temperature parameters depending on modeling momentum transfer. It has been deemed that Schmidt and Prandtl numbers are equal for current turbulent and reacting flow [2].

The effects of different Schmidt numbers on temperature and velocity fields have been studied in this section. Schmidt numbers have been plotted as 0.3, 0.5, 0.7 and 0.9. Temperature-velocity profiles on horizontal and vertical lines and temperature-velocity contours on midplane have been shown to examine the effects of different scenarios on the flow field.

It has been observed that the Schmidt number does not significantly affect the velocity field in Figure 12 and Figure 13. When looking at temperature contours in Figure 12, as Schmidt number increase, it is seen that temperature values in high-temperature region decrease to a certain extent in radial and axial directions. Especially for temperature profiles in Line 1, Line 2, and Line 3 graphs displayed in Figure 13, the drop of temperatures based on the increase in Schmidt number stands out. When looking at line 4 and line 5 graphs, it is seen that there are no significant changes. When Schmidt numbers are compared with experimental results, it is observed that taking Schmidt number as 0.7 provides more logical results.

In addition, the average temperature value at the exit of the combustion chamber for 0.3, 0.5, 0.7, and 0.9 values of Schmidt number have been calculated as 1000 K, 1003 K, 1005 K and 1007 K, respectively. This situation indicates that the average temperature value at the exit of the combustion chamber increases insignificantly as the Schmidt number increase.

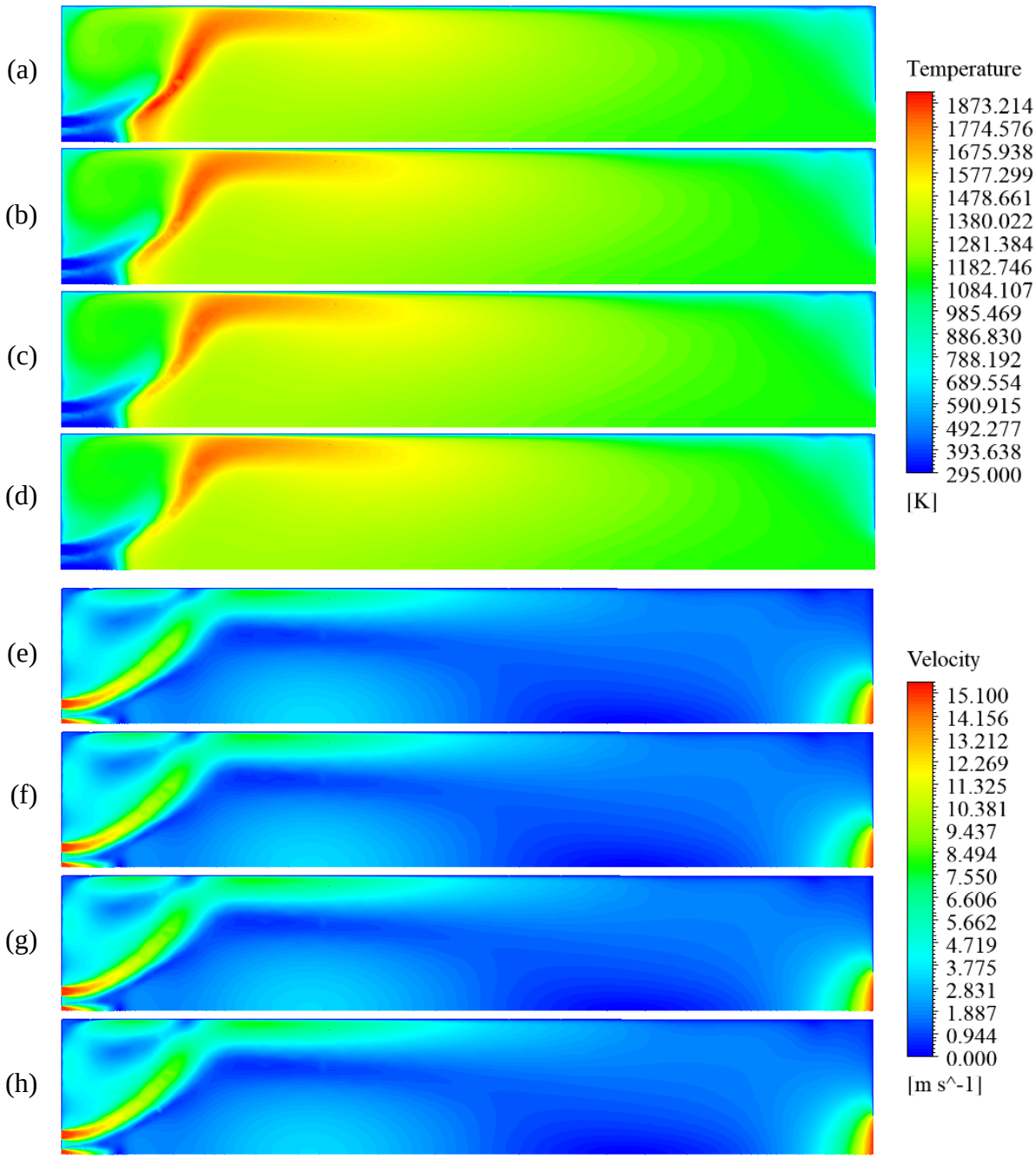

Figure. 12. Contours showing temperature fields for (a) Sch=0.3 (b) Sch=0.5 (c) Sch=0.7 (d) Sch=0.9 and velocity fields for (e) Sch=0.3 (f) Sch=0.5 (g) Sch=0.7 (h) Sch=0.9.

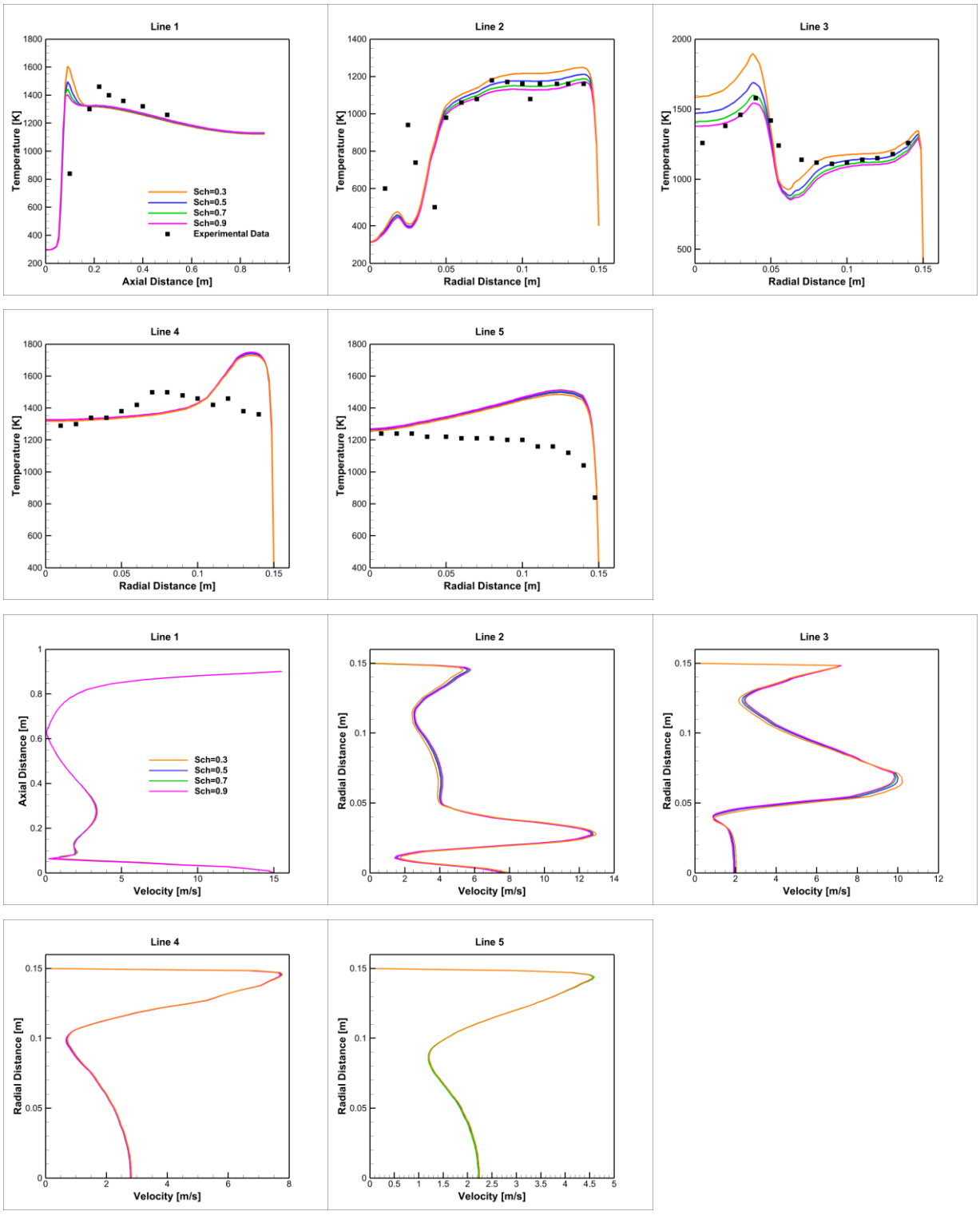

Figure 13. Temperature and velocity profiles on horizontal and vertical lines created for the study of the effect of turbulent Schmidt number.

5.5. Effect of radiation heat transfer

In order to examine the effects of radiation heat transfer modeling on the temperature field, the combustion chamber has been addressed in 2 different ways in this section: scenario with radiation and scenario without radiation. In the scenario with radiation, discrete ordinates (DO) is used to account for radiation heat transfer, while radiation heat transfer is not considered in the scenario without radiation. Temperature contours on the midplane and temperature profiles on horizontal and vertical lines have been presented to investigate the impact of different scenarios on the temperature field.

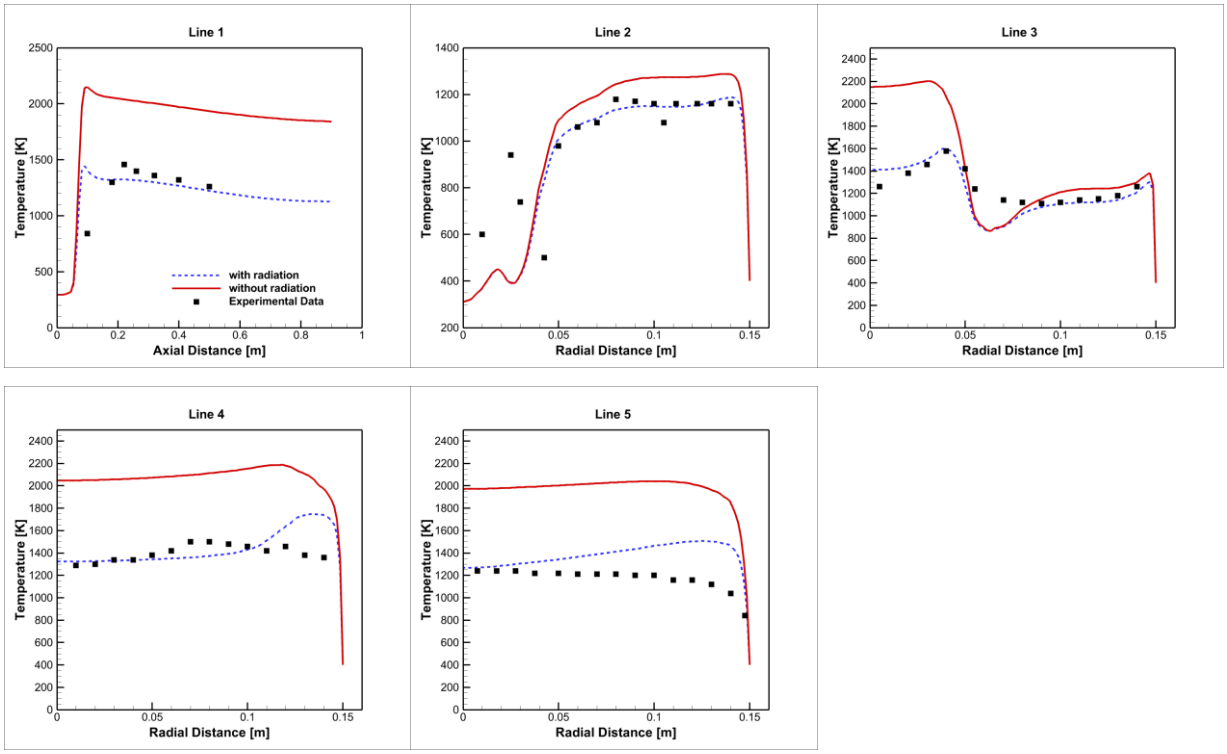

Figure 14. Temperature profiles on horizontal and vertical lines created for the study of the effect of radiation heat transfer.

According to the results obtained, it is observed that radiation heat transfer has a significant effect on the temperature field. For temperature profiles in Figure 14, the distribution of temperature values in the study conducted without considering radiation heat transfer decrease when radiation heat transfer is taken into account. Hence distributions with lower temperature values have appeared in the scenario with radiation. In other words, calculations involving only convection heat transfer appear to overestimate temperature levels.

For temperature contours in Figure 15, the scenario without radiation has produced a structure with more high-temperature zones. The reason for the formation of distribution with lower temperature values in the scenario with the radiation compared to the scenario without radiation is rooted in more heat transfer from hot gases to combustion chamber walls, which makes radiation heat transfer more important than convection heat transfer in numerical simulations conducted for the combustion chamber.

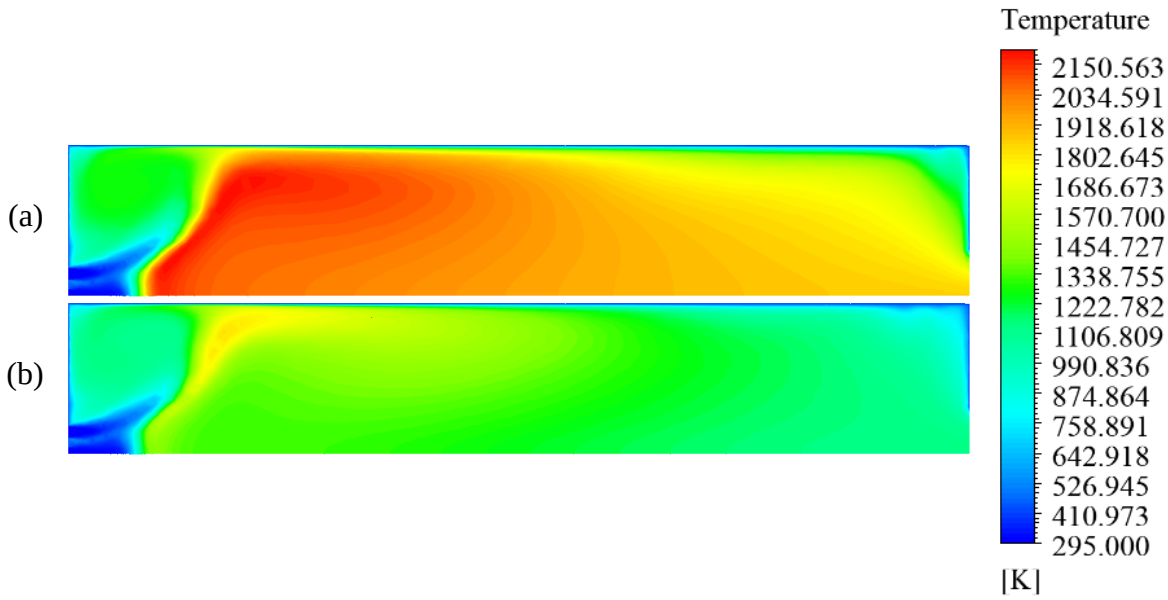

Fig. 15. Contours showing temperature areas of scenarios (a) without radiation and (b) with radiation.

As seen in Table 6, considering radiation heat transfer has caused a decrease in temperatures on observation points. In particular, while the temperature value of Point 9 is higher than 2000 K before radiation heat transfer takes into, it has reached a temperature value less than 1500 K after radiation heat transfer takes into account. As a result, it stands out that the scenario with radiation is highly compatible with experimental results.

Table 6. It shows the variation of maximum temperature values on observation points after considering radiation heat transfer.

	Without radiation	With radiation
Point 1	1011.9019 K	932.86835 K
Point 2	1270.3934 K	1129.5646 K
Point 3	1395.2092 K	1251.2117 K
Point 4	2073.3418 K	1343.899 K
Point 5	2003.0502 K	1344.4063 K
Point 6	1803.1279 K	1143.1143 K
Point 7	1705.3553 K	1116.1267 K
Point 8	2041.4047 K	1464.8589 K
Point 9	2153.8499 K	1428.994 K
Point 10	1209.6246 K	1095.156 K

6. CONCLUSIONS

This study presents a numerical investigation of momentum, heat transfer, and combustion mechanisms of non-premixed swirling flame movement of a cylindrical combustion chamber. Fluent, a commercial CFD software, has been used in calculations. The results underline the following conclusions:

Realizable k-epsilon has proved more feasible in estimating temperature-velocity profiles and contours in the turbulence modeling study. When numerical results are compared with experimental results, it is seen that realizable k-epsilon produces results with more accuracy. In addition, it has been observed that realizable k-epsilon provides ease of convergence by eliminating numerical difficulties compared to SST k-omega, offering similar results in modeling reacting flow. However, it has been discovered that standard k-epsilon gives better results in some parts of the combustion chamber where realizable k-epsilon is insufficient. Standard k-omega and RNG k-epsilon have estimated temperature and velocity fields differently from other turbulence models. This situation cause desired results in predicting flame structure, recirculation zones and flow separations.

In the combustion modeling study, FR/EDM-4 step generally presents results in agreement with experimental data for the temperature field. SDFM-GRI Mech 3 has not been preferred in subsequent studies in terms of length of simulation time and incompatibility with experimental results. In addition, SDFM-GRI Mech 3 has failed to predict the velocity field towards the exit of the furnace.

FR/EDM-3 step has presented more compatible results with experimental results in the Line 5 graph. EDM-1 step and FR/EDM-4 step offer more acceptable results in estimating temperature values in the centerline. It has emerged contours with generally similar high-temperature distributions in CRZ for EDM-1 step, FR/EDM-3 step and SDFM-GRI Mech 3, in IRZ for EDM-1 step and FR/EDM-4 step, towards the combustion chamber exit for EDM-1 step, FR/EDM-3 step and FR/EDM-4 step.

In the radiation modeling study, the scenario with radiation has reduced peak temperatures in the scenario without radiation and presented a structure with lower temperature values in the combustion chamber. While peak temperature in the combustion chamber is 2259 K in the scenario without radiation, it is calculated as 1897 K in the scenario with radiation. Again, while the average temperature at the combustion chamber exit is 1518 K in the scenario without radiation, this value is estimated as 1005 K in the scenario with radiation. Considering radiation heat transfer causes an increase in heat transfer from the combustion chamber, which provides desired agreement with experimental results.

In the study of turbulent Schmidt number, it has been observed that as Schmidt number increases, the flame temperatures decrease to a certain extent in the combustion chamber. Taking Schmidt number as 0.7 for the combustion chamber increases accuracy in estimating the temperature field. In addition, it has been seen that the Schmidt number does not significantly affect the velocity field. Finally, it is seen that the average temperature value at the exit of the combustion chamber increases insignificantly as the Schmidt number increase.

While standard k-epsilon was applied as turbulence model in studies in Ref. [6], [8] and [12], realizable k-epsilon was applied in Ref. [13]. While applying eddy dissipation with the 1-step reaction mechanism as combustion model in studies in Ref. [6] and [8], probability density function/mixture fraction was applied in Ref. [12] and [13]. While applying discrete ordinates as radiation model in the study in Ref. [12], P1 was applied in Ref. [6], [8] and [13]. Realizable k-epsilon, a combination of FR/ED with the 4-step reaction mechanism, and DO have been applied as turbulence, combustion and radiation model in this study. It has been observed that previous studies could not capture oscillations in temperature profiles. This study makes a significant difference in capturing oscillations in temperature profiles, especially for Line 2 and Line 3.

Acknowledgment

The authors gratefully acknowledge Erciyes University for using the Ansys Fluent code.

Declaration of Ethical Standards

The authors declare that there is no conflict of interest regarding the publication of this paper.

Contribution of the Authors

Fatih Eker: Methodology, Conceptualization, Investigation, Software, Validation, Formal analysis, Writing - Original Draft, Writing - Review & Editing, Visualization, Resources.
İlker Yılmaz: Methodology, Conceptualization, Investigation, Supervision, Writing - Original Draft, Writing - Review & Editing, Visualization, Resources.

REFERENCES

[1] Silva, C., V., França, F., H., R., Vielmo, H., A. "Analysis of the turbulent, non-premixed combustion of natural gas in a cylindrical chamber with and without thermal radiation", *Combustion Science and Technology* 2007:179(8);1605-1630.

[2] Jiang, L., Y., Campbell, I. "Prandtl/Schmidt number effect on temperature distribution in a generic combustor", *International Journal of Thermal Sciences* 2009:48(2);322-330.

[3] Yang, X., He, Z., Qiu, P., Dong, S., Tan, H. "Numerical investigations on combustion and emission characteristics of a novel elliptical jet-stabilized model combustor", *Energy* 2019:170;1082-1097.

[4] Solmaz, M., B., Uslu, S., Uzol, O. "Unsteady RANS for simulation of high swirling non-premixed methane-air flame", *50nd American Institute of Aeronautics and Astronautics Joint Propulsion Conference* Cleveland, OH, 2014.

[5] Keramida, E., P., Liakos, H., H., Founti, M., A., Boudouvis, A., G., Markatos, N., C. "The discrete transfer radiation model in a natural gas-fired furnace", *International Journal for Numerical Methods in Fluids* 2000:34(5);449-462.

[6] Yılmaz, İ. "Effect of swirl number on combustion characteristics in a natural gas diffusion flame", *Journal of Energy Resources Technology* 2013:135(4);042204.

[7] Bahramian, A., Maleki, M., Medi, B. "CFD modeling of flame structures in a gas turbine combustion reactor: velocity, temperature, and species distribution", *International Journal of Chemical Reactor Engineering* 2017:15(4);20160076.

[8] Hosseini, A., A., Ghodrat, M., Moghiman, M., Pourhoseini, S., H. "Numerical study of inlet air swirl intensity effect of a methane-air diffusion flame on its combustion characteristics", *Case Studies in Thermal Engineering* 2020:18;100610.

[9] Silva, C., V., Deon, D., L., Centeno, F., R., França, F., H., R., Pereira, F., M. "Assessment of combustion models for numerical simulations of a turbulent non-premixed natural gas flame inside a cylindrical chamber", *Combustion Science and Technology* 2018:190(9);1528-1556.

[10] Saygin, Y., Uslu, S. "Effect of radiation on gas turbine combustor liner temperature with conjugate heat transfer (CHT) methodology", *52nd American Institute of Aeronautics and Astronautics Joint Propulsion Conference* Salt Lake City, UT, 2016.

[11] Benim, A., C., Iqbal, S., Nahavandi, A., Wiedermann, A., Meier, W., Joos, F. "Analysis of turbulent swirling flow in an isothermal gas turbine combustor model", *Proceedings of the ASME Turbo Expo 2014: Turbine Technical Conference and Exposition Volume 4A: Combustion, Fuels and Emissions* Düsseldorf, Germany, 2014.

[12] Yang, X., He, Z., Niu, Q., Dong, S., Tan, H. "Numerical analysis of turbulence radiation interaction effect on radiative heat transfer in a swirling oxyfuel furnace", *International Journal of Heat Mass Transfer* 2019:141;1227-1237.

[13] İlbaş, M., Karyeyen, S., Yilmaz, İ. "Effect of swirl number on combustion characteristics of hydrogen-containing fuels in a combustor", *International Journal of Hydrogen Energy* 2016:41(17);7185-7191.

[14] Benim, A., C., Iqbal, S., Meier, W., Joos, F., Wiedermann, A. "Numerical investigation of turbulent swirling flames with validation in a gas turbine model combustor", *Applied Thermal Engineering* 2017:110;202–212.

[15] Yılmaz, İ., Taştan, M., İlbaş, M., Tarhan, C. "Effect of turbulence and radiation models on combustion characteristics in propane–hydrogen diffusion flames", *Energy Conversion and Management* 2013:72;179-186.

[16] Garcia, A., M., Rendon, M., A., Amell, A., A. "Combustion model evaluation in a CFD simulation of a radiant-tube burner", *Fuel* 2020:276;118013.

[17] İlbaş, M., Bektas, A., Karyeyen, S. "A new burner for oxy-fuel combustion of hydrogen containing low-calorific value syngases: An experimental and numerical study", *Fuel* 2019:256;115990.

[18] Tyliszczak, A., Boguslawski, A., Nowak, D. "Numerical simulations of combustion process in a gas turbine with a single and multi-point fuel injection system", *Applied Energy* 2016:174;153-165.

[19] Yilmaz, H., Cam, O., Tangoz, S., Yilmaz, I. "Effect of different turbulence models on combustion and emission characteristics of hydrogen/air flames", *International Journal of Hydrogen Energy* 2017:42(40);25744-25755.

[20] Zhiyin, Y. "Large-eddy simulation: Past, present and the future", *Chinese Journal of Aeronautics* 2015:28(1);11–24.

[21] Salim, S., M., Cheah, S. "Wall y + strategy for dealing with wall-bounded turbulent flows", *Proceedings of the International MultiConference of Engineers and Computer Scientists Vol II* Hong Kong, 2009.

[22] Acampora, L., Marra, F., S., Martelli, E. "Comparison of different CH4-Air combustion mechanisms in a perfectly stirred reactor with oscillating residence times close to extinction", *Combustion Science and Technology* 2016:188(4-5);707-718.

[23] Guessab, A., Aris, A., Bounif, A., Gökalp, I. "Numerical analysis of confined laminar diffusion flame - effects of chemical kinetic mechanisms", *International Journal of Advanced Research in Education and Technology* 2013:4(1);59-78.

[24] Smith, G., P. et al., "GRI-Mech 3.0." [Online]. Available: http://combustion.berkeley.edu/gri-mech/version30/text30.html

[25] ANSYS Inc., ANSYS Fluent Theory Guide 18.0, Canonsburg, PA, USA, 2017.

[26] Spangelo, Ø. "Experimental and theoretical studies of a low NO_X swirl burner", *PhD Thesis*, The Norwegian University of Science and Technology, 2004.

[27] ANSYS Inc., Introduction to ANSYS Fluent for 17.0 - Module 07: Heat Transfer, Canonsburg, PA, USA, 2016.

[28] ANSYS Inc., Introduction to ANSYS Fluent for 17.0 - Module 08: Turbulence, Canonsburg, PA, USA, 2016.

[29] ANSYS Inc., ANSYS Fluent User's Guide 19.2, Canonsburg, PA, USA, 2018.